Biofunctionalized Protein Resistant Oligo(ethylene glycol)-Derived Polymer Brushes as Selective Immobilization and Sensing Platforms

Jelena Trmcic-Cvitas,[†] Erol Hasan,[†] Madeleine Ramstedt,[†,‡] Xin Li,[§] Matthew A. Cooper,[§,||] Chris Abell,[*,†] Wilhelm T. S. Huck,[†] and Julien E. Gautrot[*,†]

Department of Chemistry, University of Cambridge, Lensfield Road, Cambridge, CB2 1EW, United Kingdom, Department of Chemistry, Umeå University, SE-90187 Umeå, Sweden, Cambridge Medical Innovations, 181 Cambridge Science Park, Cambridge CB4 0GJ, United Kingdom, and Institute for Molecular Biosciences, University of Queensland, Brisbane, 4072, Australia

Received June 22, 2009; Revised Manuscript Received August 27, 2009

Poly(oligo(ethylene glycol) methacrylate) (POEGMA) brushes are extremely protein resistant polymer coatings that can reduce nonspecific adsorption of proteins from complex mixtures such as blood, sera and plasma. These coatings can be prepared via atom transfer radical polymerization with excellent control of their thickness and grafting density. We studied their direct functionalization with streptavidin and developed an assay for determining which coupling conditions afford the highest streptavidin loading efficiency. Disuccinimidyl carbonate was found to be the most efficient activating agent for covalent capture of the receptor. Using infrared and X-ray photoelectron spectroscopy, fluorescence microscopy, surface plasmon resonance, and ellipsometry, we examined how structural parameters such as the length of the oligo(ethylene glycol) side chain affect streptavidin functionalization, but also immobilization of biotinylated antibodies, subsequent selective secondary recognition and nonspecific binding of proteins. We found evidence that large macromolecules cannot infiltrate dense polymer brushes and that bulky antibody recognition occurs in the upper part of these coatings.

Introduction

The control of biomaterials surface properties, binding capacity, and specific recognition is essential for the development of functional coatings to be used in biosensing and medical diagnostics,[1−3] heterogeneous biocatalysis,[4,5] and cellular patterning.[6,7] In these applications, the moieties and molecules involved in the recognition and binding events are critical, but the physical and structural properties of coatings equally play an important role in preserving protein functional structure,[8] directing their sensing pockets in optimal orientations,[9,10] achieving high loading capacity,[11] and limiting nonspecific binding of undesired proteins and molecules.[12,13] In this respect, polymer brushes are extremely attractive coatings because their molecular structure, size, grafting density, and responsive properties can be controlled precisely. Routine preparation of these coatings was enabled by the development of controlled radical polymerizations, such as those mediated by nitroxides, RAFT agents, or atom transfer via metal catalysts, which allow the accurate control of the brush layer thickness, density, and polydispersity.[14,15]

In particular, poly(ethylene glycol) derived polymer brushes can be synthesized with great reproducibility.[16,17] Their packing density and molecular structure confer to these materials exceptional protein resistance and functional moieties that can take part in biomolecule immobilization. Indeed, poly(oligo(ethylene glycol) methacrylate) (POEGMA) brushes have been showed to preserve their nonfouling properties even in the presence of concentrated complex mixtures such as sera and plasma. This is an advantage compared to other types of platforms currently used for biosensing and medical diagnostics such as those based on self-assembled monolayers (SAMs) or dextran.[12,18,19]

However, the selective decoration of POEGMA brushes with proteins remains particularly challenging: the extreme protein repellence of POEGMA does not favor biofunctionalization, which requires large macromolecules to reside for a sufficient length of time close to activated functional groups to promote covalent or stable immobilization. Klok and co-workers have shown that by using selective and efficient couplings based on reaction of a benzylguanine moiety with an AGT fusion protein, selective biofunctionalization can be achieved.[20] Choi and co-workers opted for the covalent coupling of small molecules such as biotin via click chemistry or esterification and subsequent immobilization of streptavidin (SA).[21,22] SA/biotin binding is a particularly attractive immobilization method, owing to its extremely high association constant and the availability of a wide range of biotinylated proteins, antibodies and DNA strands.[23] Therefore, direct SA functionalization of protein-resistant polymer brushes would be highly desirable as it would enable the preparation of selective coatings with high binding capacity for biomedical applications. To achieve the preparation of such coatings, we developed a simple fluorescence assay that allowed us to determine efficient coupling conditions for high loading of SA molecules in PEG-derived polymer brushes. We further explored how the PEG side-chain length of the resulting brushes affects levels of immobilized SA as well as the binding of biotinylated antibodies and subsequent secondary recognition events.

* To whom correspondence should be addressed. E-mail: jeg45@cam.ac.uk (J.E.G.); ca26@cam.ac.uk (C.A.).
[†] University of Cambridge.
[‡] Umeå University.
[§] Cambridge Medical Innovations.
[||] University of Queensland.

10.1021/bm900706r CCC: $40.75
Published on Web 09/17/2009

Experimental Section

Materials. Oligo(ethylene glycol methacrylate) (OEGMA-360, M_w 360 and OEGMA-526, M_w 526), 2-hydroxyethyl methacrylate (HEMA), CuCl, $CuBr_2$, 2,2′-dipyridyl (bpy), succinic anhydride, glutaric anhydride, *N*-hydroxysuccinimide (NHS), 1-ethyl-3-(3-dimethylaminopropyl)carbodiimide hydrochloride (EDC), pentafluoropyridine, 3-chloropropionaldehyde diethylacetal, 4-nitrophenyl chloroformate, tresyl chloride, oxalyl chloride, cyanuric chloride, carbonyldiimidazole (CDI), triflic anhydride, disuccinimidyl carbonate (DSC), 4-(dimethylamino)pyridine (DMAP), triethylamine, diisopropylethylamine (DIEA), dimethylformamide (DMF), tetrahydrofuran (THF), methoxyethanolamine, *N*-biotinyl-3-aminopropylammonium trifluoroacetate (**1**), streptavidin, chromeon 546-streptavidin, bovine serum albumin (≥96%, cell culture tested grade), and phosphate-buffered saline (PBS, 150 mM) were purchased from Aldrich and used as received. Fetal bovine serum (FBS) Gold was purchased from PAA laboratories. A biotinylated rabbit-antigoat (bt-Rb-α-Gt) antibody was obtained from Daco. Goat-antirat (Gt-α-Rt) and donkey-antirat (Dk-α-Rt) antibodies tagged with an Alexa Fluor 488 nm excitation dye were purchased from Invitrogen. ω-Mercaptooctylbromoisobutyrate (**2**) was synthesized following a method adapted from the literature for the parent undecyl derivative.[14,24,25] Deionized water was obtained using a Synergy system from Millipore. Silicon wafers (Compart Technology Ltd.) were coated with chromium (15 nm) and gold (200 nm, Birmingham Metal) using an Edwards Auto 500 evaporator. For sample preparation, gold-coated wafers were cut in 1 cm^2 squares.

Polymer Brush Growth. For the growth of a 30 nm thick POEGMA-360 brush: a solution of $CuBr_2$ (9 mg, 40 μmol), bpy (160 mg, 1.0 mmol), and OEGMA-360 (6.3 g, 17.5 mmol) in water (11 mL) was degassed using nitrogen bubbling for 30 min. CuCl (41 mg, 410 μmol) was added to this solution, and the resulting mixture further degassed for 10 min before transferring to a flask containing the initiator-coated gold surface (immersion in 5 mM ethanolic solution of ω-mercaptooctylbromoisobutyrate overnight) under inert atmosphere. The polymerization was stopped after 30 min by immersing the coated surface in deionized water and subsequently washed with copious amounts of ethanol before drying in a nitrogen stream.

For the growth of a 30 nm thick POEGMA-526 brush: similarly as for POEGMA-360 brushes, using a solution of $CuBr_2$ (9 mg, 40 μmol), bpy (160 mg, 1.0 mmol), and OEGMA-526 (6.3 g, 12.0 mmol), water (11 mL), CuCl (41 mg, 410 μmol), and a polymerization time of 45 min.

For the growth of a 30 nm thick PHEMA brush: similarly as for POEGMA brushes, using a solution of $CuBr_2$ (9 mg, 40 μmol), bpy (160 mg, 1.0 mmol), and HEMA (6.3 g, 48.4 mmol), water (11 mL), CuCl (41 mg, 410 μmol), and a polymerization time of 10 min.

Polymer Brush Activation. All activations were carried out under an inert atmosphere.

A. Succinic and Glutaric Anhydride for EDC/NHS Activation. Brush-coated chips were incubated in THF (anhydrous, 2 mL) with the corresponding anhydride (100 mg) and triethylamine (100 μL, 0.71 mmol). They were heated for 18 h at 60 °C, washed with THF and water, and then dried in a stream of nitrogen. The resulting chips were activated in an aqueous solution (1 mL) of EDC (75 mg, 0.39 mmol) and NHS (13 mg, 0.11 mmol) for 1 h, washed briefly with deionized water, and immediately used for immobilization.

B. Pentafluoropyridine. Brush-coated chips were incubated in THF (1 mL) with DIEA (120 μL, 0.69 mmol) for 30 min. A solution of pentafluoropyridine (120 mg, 0.71 mmol) in THF (1 mL) was added, and the mixture was left to react for 3 h at room temperature. The chips were washed with THF and sonicated in THF and dried in a stream of nitrogen.

C. 3-Chloropropionaldehyde Diethylacetal. Brush-coated chips were incubated in THF (2 mL) and triethylamine (100 μL, 0.71 mmol) for 30 min. 3-Chloropropionaldehyde diethylacetal (100 mg, 0.60 mmol) was added, and the mixture was left to react for 3 h at room temperature. Hydrolysis of the resulting acetal-brush was performed using 10% HCl for 15 min and chips were washed with THF and sonicated in THF and water, and dried in a stream of nitrogen.

D. Nitrophenyl Chloroformate. Brush-coated chips were incubated in a THF (anhydrous, 2 mL) solution of nitrophenyl chloroformate (100 mg, 0.5 mmol) and triethylamine (35 μL, 0.25 mmol). A white precipitate formed. After reacting for 18 h, the chips were washed with THF and sonicated in THF before drying in a stream of nitrogen.

E. Tresyl Chloride. Brush-coated chips were incubated in THF (2 mL) with triethylamine (120 μL, 0.85 mmol) for 30 min before addition of tresyl chloride (83 mg, 0.45 mmol). The resulting mixture was left to react for 3 h at room temperature. The chips were washed with THF, sonicated in THF, and dried in a stream of nitrogen.

F. Oxalyl Chloride. Brush-coated chips were incubated in THF (2 mL) with triethylamine (120 μL, 0.85 mmol) for 30 min before oxalyl chloride (83 mg, 0.65 mmol) was added. The mixture was left to react for 3 h at room temperature, and the chips were washed with THF and sonicated in THF before drying in a stream of nitrogen.

G. Cyanuric Chloride. Brush-coated chips were incubated in THF (1 mL) with DIEA (180 μL, 1.04 mmol) for 30 min before adding a solution of cyanuric chloride (100 mg, 0.54 mmol) in THF (1 mL). The resulting mixture was left to react for 3 h at room temperature, and the chips were washed with THF, sonicated in THF, and dried in a stream of nitrogen.

H. Carbonyldiimidazole (CDI). Brush-coated chips were incubated in THF (2 mL) with CDI (100 mg, 0.62 mmol) for 18 h at room temperature. Chips were washed with THF and dried in a stream of N_2.

I. Triflic Anhydride. Brush-coated chips were incubated in pyridine (2.5 mL) in an ice bath and triflic anhydride (75 μL, 0.45 mmol) was added. The reaction mixture was left to react for 1 h at 0 °C and then at room temperature for 1 h. Chips were washed with pyridine and water and dried in a stream of nitrogen.

J. Disuccinimidyl Carbonate (DSC). Brush-coated chips were incubated in an anhydrous DMF (2 mL) solution containing DSC (51 mg, 0.2 mmol) and DMAP (24 mg, 0.2 mmol) under inert atmosphere, at room temperature, for 18 h. Chips were washed with DMF and water and dried in a stream of nitrogen.

Immobilization of Streptavidin. Activated brushes were incubated in a 100 μg/mL solution of SA in PBS (pH 7.4) for 15 min to 18 h. In the case of chromeon-SA immobilization, for the fluorescence assay, chips were kept in the dark. Chips were washed by incubating in PBS for 1 h. For SPR studies, chips were mounted on the plastic support before SA incubation and kept in PBS after immobilization. For fluorescence assays, chips were washed with PBS and deionized water, and dried in a stream of nitrogen. Fluorescence measurements were carried out immediately.

Biotinylation. Activated brushes were incubated in a 5 mg/mL solution of amino-biotin **1** in PBS (pH 7.4) for 18 h, washed in deionized water for 1 h and dried in a stream of N_2. Subsequent streptavidin binding was carried out in a streptavidin solution (10 μg/mL) for 15 min. Finally, brushes were incubated in PBS for 30 min, washed with deionized water, and dried in a stream of nitrogen.

Instrumental Analyses. Fluorescence measurements were carried out on a Leica DMI 4000B microscope, with a CTR 6000 laser (excitation filter BP480/40, suppression filter B527/30, dichromatic mirror 505). All images were recorded with identical settings (laser intensities and gains) at five incremental exposure times, to allow a wider intensity window to be probed. Measurements were carried out in triplicate, at three distant positions for each sample (average of nine values). The level of background (nonfunctionalized areas) was subtracted. Micropatterned substrates were prepared by microcontact printing of the ATRP thiol initiator 2 using a PDMS stamp, followed by brush growth and functionalization.[26,27]

Grazing angle FT-IR spectra were obtained on a Vertex 70 (Bruker) equipped with a MCT detector and a Veemax II stage (Pike Technologies) with an angle of incidence of 80°. A number of 64 scans were acquired in normal atmosphere for each sample. A new background

was acquired before each scan to account for small changes in the atmospheric composition. Spectra were collected from brushes grown from gold surfaces.

X-ray photoelectron spectroscopy (XPS) analyses were performed using a Kratos Axis Ultra under monochromatic Al Kα radiation (1486.6 eV). Pass energy of 160 eV and a step size of 1 eV were used for survey spectra. For high energy resolution spectra of regions a pass energy of 20 eV and a step size of 0.1 eV were used. Charging neutralizing equipment was used to compensate sample charging, and the binding scale was referenced to the aliphatic component of C1s spectra at 285.0 eV. The concentrations obtained (error less than ± 10%) are reported as the percentage of that particular atom species (at %) at the surface of the sample (<10 nm analysis depth) without any correction. The analysis area (0.3 × 0.7 mm), the angle of incidence and the beam intensity were kept constant for all measurements. In addition, the samples were assumed to be homogeneous and with similar densities in the dry state, which should allow a direct correlation between N at % and SA coverage density of the analysis area for the different brushes presently studied.

Surface plasmon resonance (SPR) was performed on a Biacore 3000. SPR chips (Ssens) were coated with the desired polymer brush (30 nm) and functionalized with SA prior to mounting on a substrate holder. Mounted chips were docked, primed with buffer (PBS) twice, and equilibrated at 20 μL/min for 30 min or until a stable baseline was obtained. For immobilization of a biotinylated antibody and sensing of a secondary antibody, the programmed sequence was the following: wash with PBS and equilibrate for 5 min, expose to a solution of bt-Rb-α-Gt (primary antibody) for 5 min, wash with PBS for 10 min, expose to a solution of secondary antibody (Gt-α-Rt or Dk-α-Rt) for 5 min, and wash with PBS for 10 min. For immobilization of SA on a biotinylated brush, a chip was equilibrated in PBS for 5 min, exposed to a SA solution (10 μg/mL) in PBS for 5 min, and washed with PBS for 10 min. For measurement of nonspecific binding, a chip was washed and equilibrated in PBS for 5 min, exposed to 10% FBS for 15 min and washed with PBS for 15 min. The flow rate was 20 μL/min. Measurements were carried out in triplicate.

Ellipsometry measurements were performed with a α-SE instrument from J.A. Woolam at 70° incidence angle. A simple gold substrate/cauchy film model was used and fitted between 400 and 900 nm.

Results

Streptavidin Immobilization Assay. To efficiently screen several coupling agents and conditions for the efficient immobilization of SA, a simple fluorescence assay was developed. Patterned gold substrates displaying an alternation of POEGMA-360 brush-coated areas and unprotected gold areas were prepared. Polymer brushes were activated and subsequently incubated in fluorescently tagged SA (chromeon 546-SA) solutions. Images of the resulting substrates were recorded using a fluorescence microscope and immobilization levels were determined by measuring the average fluorescence intensity on a polymer-brush coated area, compared to a nonfunctionalized area (Figure 1B). Fluorescence coming from nonspecifically adsorbed chromeon-SA on gold is quenched by energy transfer and therefore gold areas are dark, whereas polymer-brush areas display fluorescence intensities that vary as a function of the level of SA immobilization. Two types of brushes were studied: neutral brushes, which were activated directly from hydroxyl-terminated POEGMA-360, and negatively charged brushes, which were generated by treating POEGMA-360 with glutaric or succinic anhydride and activated via EDC/NHS coupling.

For direct activation of neutral brushes, disuccinimidyl carbonate (DSC) was found to be the most efficient and reliable coupling agent (Figure 2). Cyanuric chloride, carbonyldiimidazole (CDI), and triflic anhydride also afforded relatively high

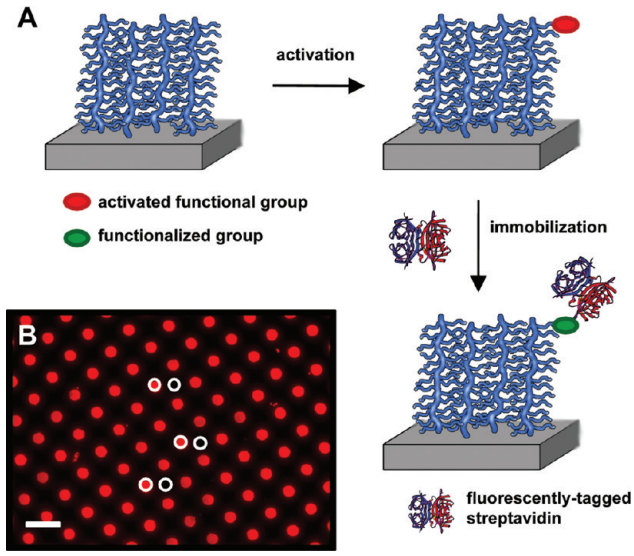

Figure 1. (A) Direct immobilization of proteins on polymer brushes in a two-step process. (B) Protein (SA bearing a fluorescent tag, chromeon 546 nm) immobilization levels were determined by fluorescence assay. The average fluorescence intensity in zones delimited by the white rings was measured for a brush coated area and a bare gold area. Scale bar: 50 μm.

levels of immobilization, although with a 2−3-fold decrease, whereas nonactivated brushes incubated with SA for identical periods of time displayed nonspecific adsorption levels 2−3 orders of magnitude lower, consistent with the nonfouling properties of POEGMA brushes. Protein resistance properties were preserved upon functionalization with glutaric anhydride, despite the presence of negative charges. However, succinate-POEGMA-360 brushes displayed a 7-fold increase in nonspecific binding (Figure 2), perhaps due to higher functionalization and lower pK_a of the resulting acid moieties. Both glutarate- and succinate-POEGMA-360 brushes afforded relatively high immobilization levels, after activation with EDC/NHS treatment, comparable to cyanuric chloride, CDI and triflic anhydride-activated brushes. However, the ratio of covalent to nonspecific immobilization was lower, due to impaired protein resistance (extrapolated from Figure 2). The higher immobilization level observed for succinate-POEGMA-360 compared to glutarate-brushes, after EDC/NHS activation presumably reflects the increased Coulombic attraction that the former surfaces generate.[28] Incubations carried out for shorter times (15 min and 1 h, Figure S1) show that NHS-activated carboxylic acid brushes react faster than most activated neutral brushes, except for those coupled with cyanuric chloride and triflic anhydride, which are known to be particularly active.[29−31] CDI and DSC-activated brushes, despite reacting more slowly, afford high SA levels due to the long lifetime of these activated groups, even in aqueous conditions.[32]

Having determined the superiority of DSC coupling for the immobilization of SA on POEGMA-360 brushes, this method of activation was used in a subsequent study of the effect of side chain length on SA coupling and binding of biotinylated antibodies. Therefore, the work further described was carried out after DSC coupling on hydroxyl-bearing polymer brushes. Brushes were directly functionalized with SA (Figure 3A) or biotinylated before incubation in SA solutions (Figure 3B). Uptake of a primary biotinylated rabbit-antigoat (bt-Rb-α-Gt) and a secondary goat-antirat (Gt-α-Rt) antibody was studied to assess the specificity of the resulting SA brushes.

Infrared Spectroscopy. The main characteristic of the IR spectrum of pristine POEGMA-360 brushes was their intense

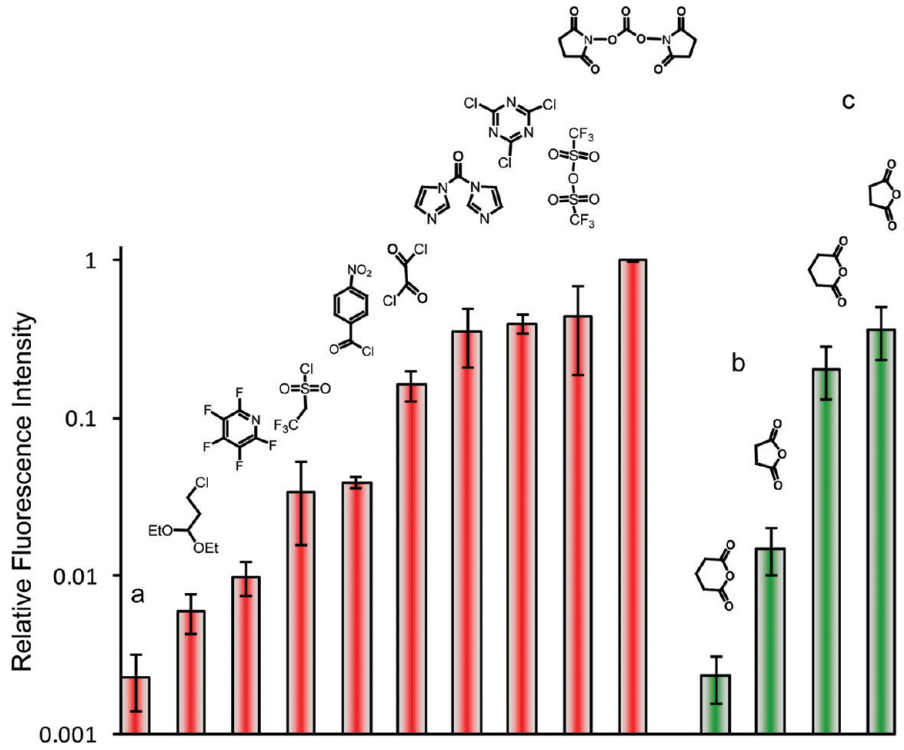

Figure 2. SA immobilization levels (determined by fluorescence assay) on POEGMA-360 brushes using a range of coupling agents. Red bars: hydroxyl-terminated brushes were directly activated with the corresponding coupling agents depicted (a, no coupling agent) before incubation for 18 h in a SA solution. Green bars: hydroxyl-terminated brushes were first functionalized with glutaric or succinic anhydride and incubated with SA (b) without NHS/EDC activation and (c) with NHS/EDC activation. Error bars represent standard deviations for $n = 3$.

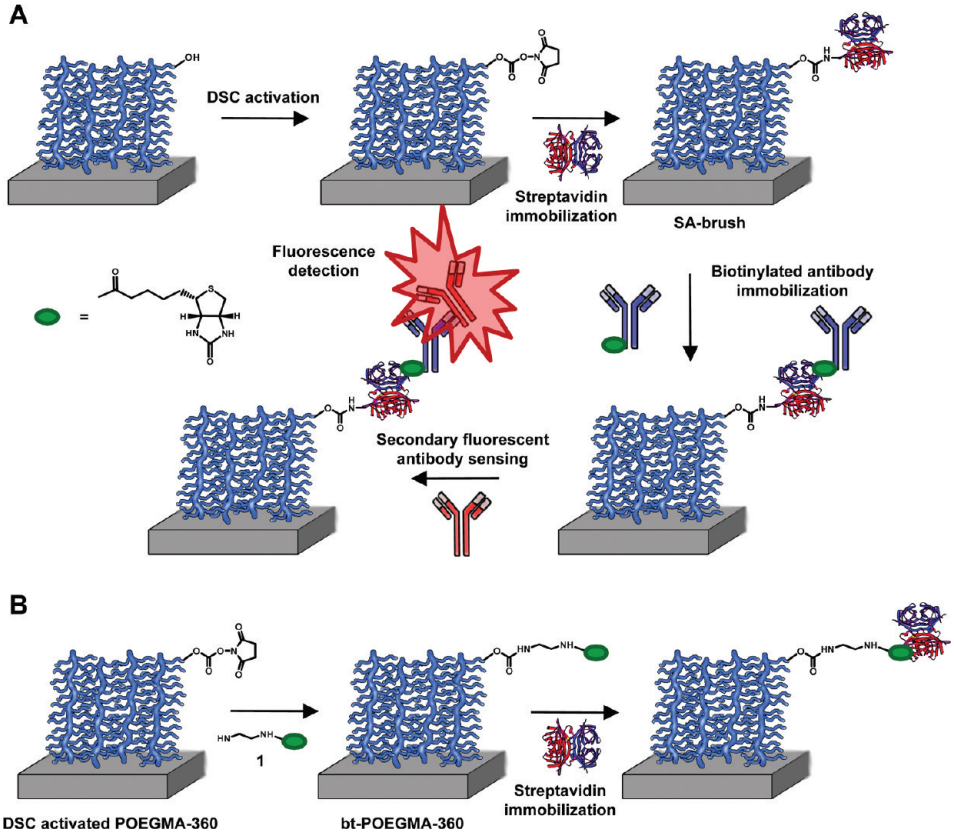

Figure 3. (A) Immobilization of biotinylated antibodies on streptavidin functionalized polymer brushes and subsequent secondary recognition. (B) Direct biotinylation of POEGMA-360 brushes and subsequent SA immobilization.

absorption at 1730 cm^{-1}, arising from carbonyl stretching (Figures 4, S2 and S3).[20] DSC-activated brushes displayed additional bands at 1790 and 1805 cm^{-1} arising from carbonate stretching (red dashed line a, Figure 4). These peaks disappeared entirely after functionalization with biotin but not when SA was directly immobilized. This is likely due to the large size of SA,

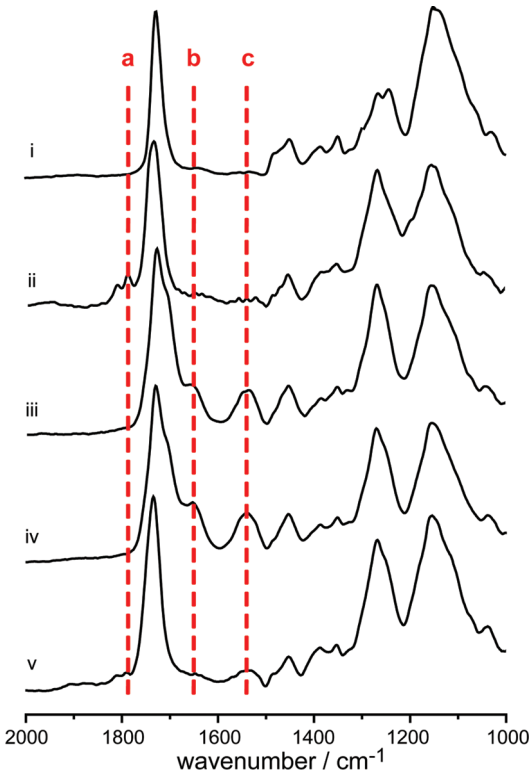

Figure 4. Grazing angle IR spectra recorded for POEGMA-360 brushes (from the top): (i) before DSC activation; (ii) after DSC activation; (iii) after biotinylation; (iv) after SA immobilization on biotinylated brushes; and (v) after direct streptavidin immobilization from DSC activated brushes. The red dashed lines correspond to the position of the bands characteristic of DSC (a), C=O stretching (b), and N-H bending (c).

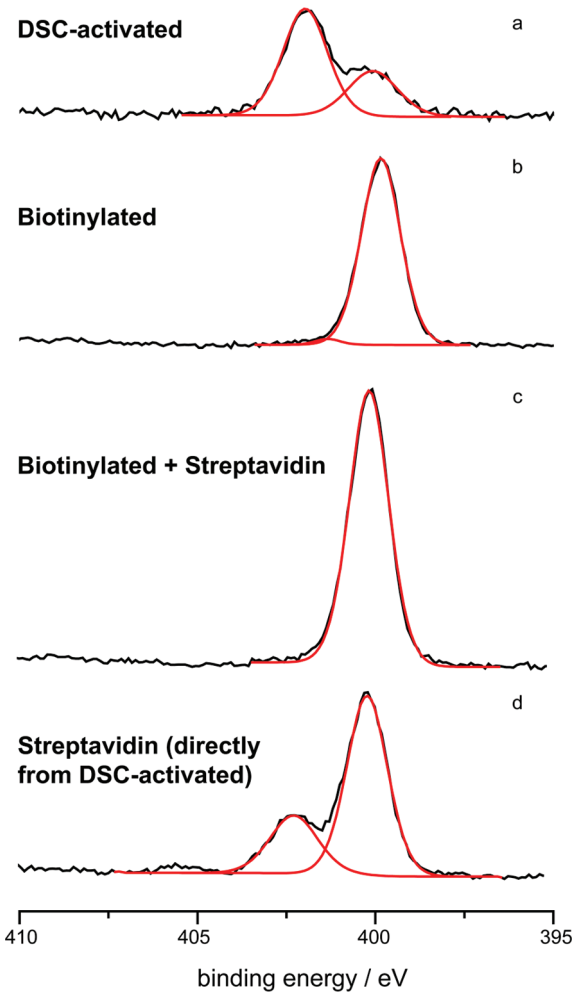

Figure 5. N XPS spectra for functionalized POEGMA-360 brushes after DSC activation (a), biotinylation (b), and streptavidin immobilization on biotinylated (c) or DSC activated brushes (d), from top to bottom respectively. Black lines: experimental data; red lines: separate peak fits.

compared to the small molecule biotin derivative used for functionalization, which does not allow this macromolecule to infiltrate fully dense polymer brushes.[33,34] The persistence of the carbonate bands also gives further evidence of the long lifetime of DSC-activated moieties in PBS,[32] consistent with the slow yet efficient coupling of SA to polymer brushes. Quenching of the remaining active functions with a small molecule amine such as methoxyethanol amine (25 mg/mL in PBS pH 8.5, 1 h) did not alter results obtained for biotinylated antibody immobilization or protein resistance, in agreement with the remaining reactive moieties being buried in the polymer brush and inaccessible to bulky macromolecules.

After exposure to SA, the IR spectrum of the resulting brushes clearly displayed new bands near 1650 and 1540 cm^{-1}, corresponding to the strong amide CO stretching and NH bending bands (red dashed lines b and c, Figure 4).[35] These bands are clearly apparent after biotinylation, consistent with the presence of amide bonds, and further increase in intensity upon incubation of the resulting biotinylated brush in a SA solution.

X-ray Photoelectron Spectroscopy (XPS). The XPS spectra of PHEMA and POEGMA brushes only display carbon and oxygen signals (with occasional traces of gold or silicon). Upon biotinylation, a clear nitrogen signal appears in the XPS spectrum of POEGMA-360 brushes (Figure 5). This signal is the sum of two components, with binding energies (BE) at 400.3 and 402.3 eV, respectively. The low BE nitrogen signal is general to most nitrogen-containing organic compounds,[36] whereas the high BE signal is specific to the succinimidyl ester (the lower BE peak in DSC-activated brushes are believed to originate from X-ray induced degradation during XPS measurement). The signal at high BE vanishes after biotinylation, whereas the low binding energy signal increases in intensity, due to the covalent immobilization of SA molecules. If DSC-activated POEGMA-360 brushes are directly incubated in SA solutions, the high BE signal does not disappear fully, suggesting that some reactive moieties remain in the brush. The SA functionalization step is particularly sensitive to the density of hydroxyl groups, i.e. the length of the oligo(ethylene glycol) side chain, as the nitrogen content of the analysis area decreases with longer chains (7.8, 2.4, and 1.5 at % for PHEMA, POEGMA-360, and POEGMA-526, respectively). Finally, biotinylated POEGMA-360 brushes gave rise to higher levels of nitrogen content (6.1 at % N) after SA incubation, in agreement with the high association constant of the biotin/SA couple (Figure 6).

In order to further test the specificity of SA-POEGMA-360 brushes, incubation was carried out in antibody solutions of decreasing concentrations (keeping the concentration of BSA constant). This resulted in a linear decrease in the level of Gt-α-Rt immobilized (Figure 7B). However, Gt-α-Rt was still detected at a concentration as low as 100 pg/mL, as the resulting antibody density was still higher than that measured after incubation in a 1 μg/mL Dk-α-Rt solution (for which the primary antibody has no specificity - red dashed line in Figure 7B).

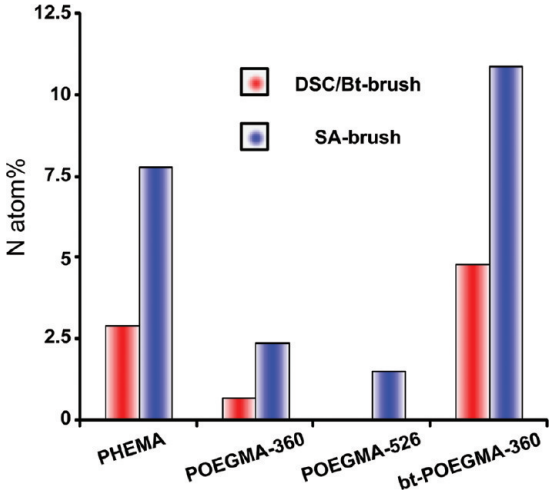

Figure 6. Nitrogen content of polymer brushes activated with DSC (PHEMA, POEGMA-360 and POEGMA-526) or biotinylated (bt-POEGMA-360) before (red) and after (blue) SA incubation, as determined by XPS.

Fluorescence Microscopy. The level of SA immobilization on the different polymer brushes was determined by fluorescence microscopy. This assay showed a clear increase in functionalization with decreasing length of side chain (POEGMA-526 ≈ POEGMA-360 < PHEMA, Figure 7A). Incubation of biotinylated brushes in SA solutions significantly increased the level of protein immobilization, consistent with XPS data. The resulting SA brushes were subsequently incubated in bt-Rb-α-Gt and finally Gt-α-Rt (tagged with a fluorescent dye) solutions (with 10% BSA). The level of secondary antibody immobilization was measured by fluorescence microscopy. Interestingly, the immobilization trends are opposite to that for SA coupling: PHEMA gives the lowest Gt-α-Rt functionalization. These observations can be rationalized by the increased nonspecific binding that characterizes oligo(ethylene glycol)-derived polymer brushes with shorter side-chains:[20,37] the antibody incubation being carried out in 10% BSA solutions, nonspecific binding competes with specific antibody recognition. These observations may also arise from potential increased crowding and over-functionalization (a process in which many reactive groups couple to one single SA molecule) in PHEMA, however, SPR results do not favor such hypothesis (see below). Hence, the specificity of SA-functionalized polymer brushes decreased with the length of the oligo(ethylene glycol) side chains.

Surface Plasmon Resonance. The immobilization of the biotinylated primary antibody and specific recognition of the secondary antibody were studied more quantitatively via SPR. The SA functionalization step could not be followed using this technique, except for biotinylated brushes bt-POEGMA-360, due to the slow rate of coupling of DSC-activated moieties. However, exposure of polymer brushes to a 10 μg/mL solution of bt-Rb-α-Gt gave rise to a clear shift in the surface bound mass of nearly 100 ng/cm^2 for POEGMA-360 (a change of 10 RU corresponds to a binding capacity of 1 ng/cm^2).[38] Exposure to a secondary Gt-α-Rt antibody (5 μg/mL solution) gave rise to a further 25 ng/cm^2 increase, whereas when Dk-α-Rt (which should not be recognized by the primary antibody) was used, a binding capacity of only 1.0 ng/cm^2 was measured (Figure 8). This confirmed the retained selectivity of biotinylated antibodies immobilized on POEGMA brushes.

The effect of varying the concentration of antibodies was then examined. The densities of both bt-Rb-α-Gt and Gt-α-Rt immobilized remained constant when the concentration of primary antibody was above 1 μg/mL (the secondary antibody concentration being kept at 5 μg/mL), suggesting that saturation of the accessible SA molecules had been achieved at this concentration (Figure 9A). Below 1 μg/mL, the binding capacities in both primary and secondary antibodies decreased to similar extents (although more for bt-Rb-α-Gt), with little infiltration of the latter macromolecules. When the concentration of the secondary antibody was varied, keeping that of bt-Rb-α-Gt constant above the plateau region, the immobilization level varied accordingly (Figure 9B), consistent with the fluorescence assay results.

The effect of side-chain length on antibody binding was studied. The density of immobilized bt-Rb-α-Gt decreased by a factor 3 with increasing side chain length (Figure 10A), consistent with both the corresponding increased protein resistance and decreased density of reactive coupling moieties. Similarly, Gt-α-Rt immobilization decreased, although only by a factor of 2, within the same series. This contrasts with fluorescence results that displayed an opposite trend. However, SPR experiments were carried out in the absence of BSA, which

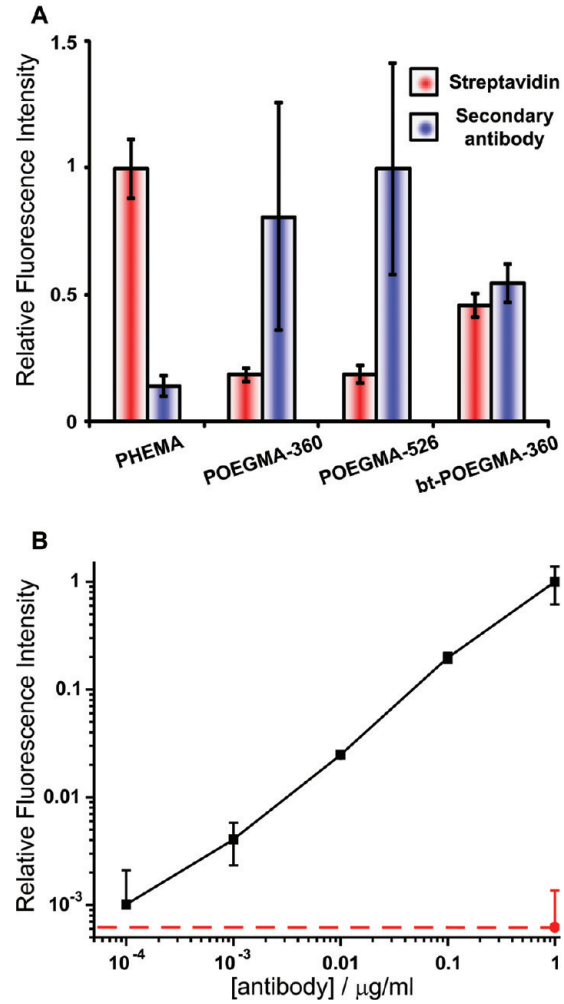

Figure 7. A) SA (after DSC-activation for PHEMA, POEGMA-360 and POEGMA-526, and after biotinylation for bt-POEGMA-360) and Gt-α-Rt secondary antibody (after brush functionalization with bt-Rb-α-Gt) immobilization levels as a function of brush type. Immobilization of antibodies was carried out in 10% BSA solutions. B) Detection of Gt-α-Rt secondary antibody immobilization on SA-POEGMA-360 brushes functionalized with bt-Rb-α-Gt (black line and squares). The level of immobilization detected for Dk-α-Rt at the highest concentration is shown in red. Error bars represent standard deviations for $n = 3$.

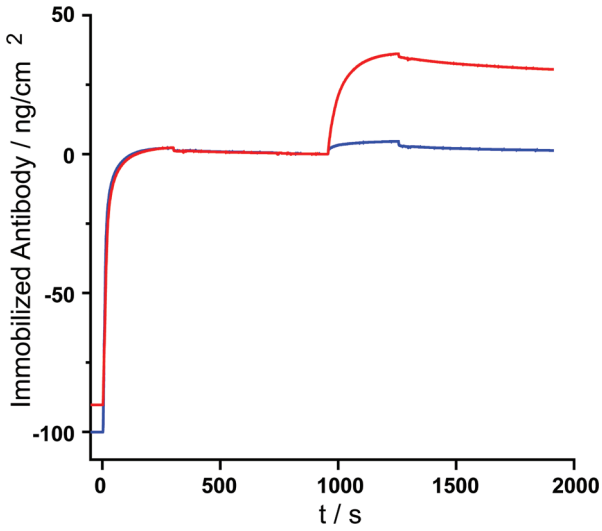

Figure 8. Functionalization of SA-POEGMA-360 brushes with bt-Rb-α-Gt (10 μg/mL) and subsequent immobilization with Gt-α-Rt (red line) or Dk-α-Rt (blue line), monitored by SPR (concentration of secondary antibodies were 5 μg/mL).

competes with specific immobilization in fluorescence experiments, in particular, with the least protein resistant brushes (e.g., PHEMA). Indeed, the level of nonspecific binding measured from a 10% FBS solution on SA functionalized brushes was significantly higher for PHEMA than for POEGMA coatings (Figure 10B). The difference between primary and secondary binding was also reflected in the marked changes in binding rates measured for the brushes studied. The initial binding rates of bt-Rb-α-Gt for PHEMA, POEGMA-360, and POEGMA-526 were 3.6, 4.4, and 2.8 ng·cm^{-2} s^{-1}, respectively, whereas those of secondary Gt-a-Rt recognition are 0.6, 0.7, and 0.8 ng·cm^{-2} s^{-1}.

Finally, the biofunctionalization of biotinylated POEGMA-360 brushes was studied for comparison with the literature (Figure 3B). Incubation in a SA solution for 5 min resulted in high immobilization densities, near 460 ng/cm^2, in excellent agreement with results reported in the literature for this type of brush.[21] However, the subsequent immobilization of bt-Rb-α-Gt was found to be less efficient, significantly below that of SA-POEGMA-360 brushes (Figure 10A). This observation presumably originates from the high biotin density of this type of brush and the resulting saturation of SA's binding pockets. Interestingly, the density of secondary antibody immobilized was unchanged compared to that obtained for SA-POEGMA-360. This further suggests that secondary antibodies do not infiltrate brushes and only interact with the uppermost layer of the coatings. This contrasts with the high SA loading levels observed for bt-POEGMA-360, implying that the smaller size of this macromolecule allows it to infiltrate polymer brushes deeper than bulky antibodies.

Discussion

Disuccinimidyl Carbonate Promotes High Streptavidin Coupling. Protein-resistant polymer brushes such as POEGMA and zwitterionic derivatives are particularly difficult to biofunctionalize because biomacromolecules do not remain in the vicinity of these coatings for long enough periods of time to react efficiently with coupling moieties. In the case of zwitterionic brushes such as poly(carboxy betains), activation of the carboxylic acid moieties with NHS esters gives rise to the

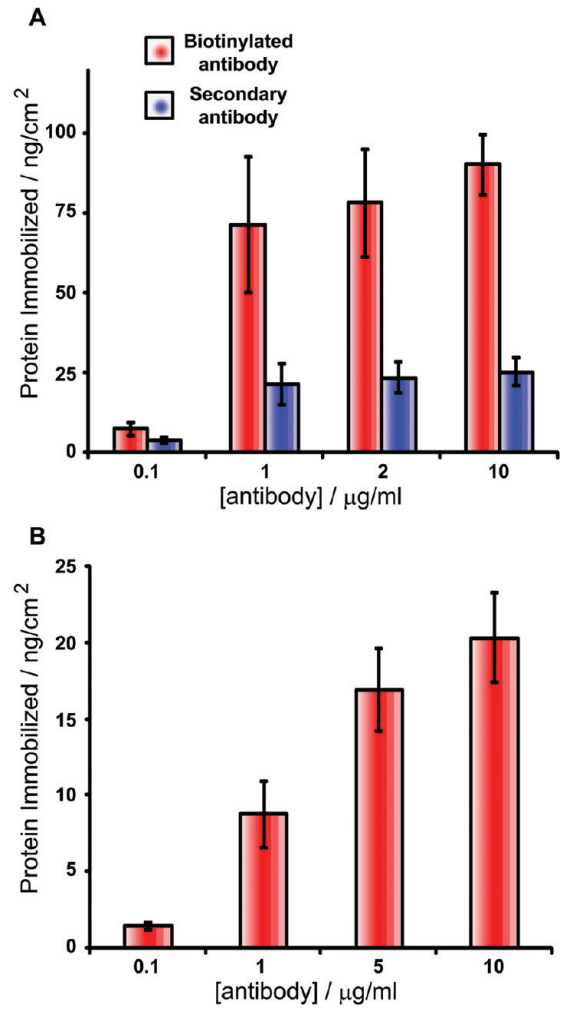

Figure 9. Antibody immobilization levels on POEGMA-360 SA-brushes, followed by SPR. (A) Levels of immobilization of bt-Rb-α-Gt and Gt-α-Rt (fixed concentration of 5 μg/mL) at different concentrations of bt-Rb-α-Gt. (B) Evolution of Gt-α-Rt immobilization in function of starting concentration, after exposure to bt-Rb-α-Gt solutions (2 μg/mL). Error bars represent standard deviations for $n = 3$.

generation of a nett positive charge that contributes to the attraction of negatively charged macromolecules via Coulombic attraction.[39,40] For neutral brushes such as POEGMA, this strategy cannot be applied and efficient coupling of large macromolecules relies on selective and efficient coupling chemistry such as the reaction catalyzed by alkylguanine-DNA-alkyltransferase with a benzylguanine-derived brush.[20] Alternatively, strong metal chelating complexes such as nitrilotriacetic acid-Ni/his-tag can be used, providing their association constant is high enough to provide stable anchoring.[41]

The fluorescence assay that we designed enabled us to screen a range of established coupling strategies for achieving high levels of immobilization of SA. Activation of negatively charged carboxylic acid-bearing polymer brushes with EDC/NHS afforded 40−70 ng/cm^2 functionalization levels (determined by comparison of the fluorescence intensity measured for SA-functionalized bt-POEGMA-360, for which a binding capacity of 460 ng/cm^2 has been determined by SPR). These moderately high immobilization levels are in good agreement with the balanced effects of low charge densities (due to the high molecular weight of the PEG side-chain) and decreased protein resistance (compared to neutral hydroxyl substituted brushes). In comparison, only four of the activating agents used with

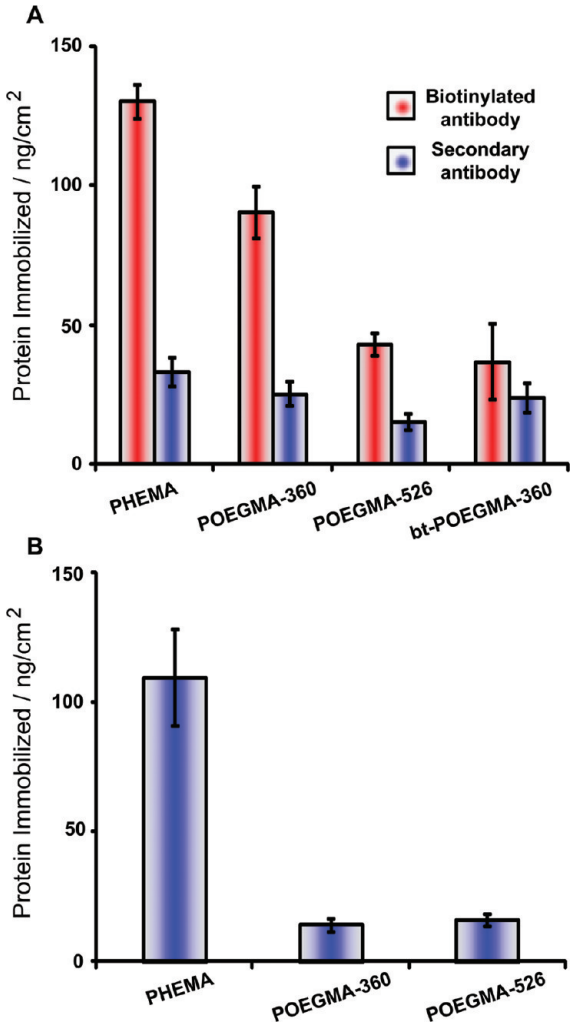

Figure 10. (A) Antibody immobilization levels on SA-brushes (biotinylated antibody: bt-Rb-α-Gt, 10 μg/mL; secondary antibody: Gt-α-Rt, 5 μg/mL). (B) Measurements of nonspecific binding to SA-brushes exposed to 10% FBS. Error bars represent standard deviations for $n = 3$.

hydroxyl-terminated brushes afforded functionalization levels above 60 ng/cm^2. These relatively high densities (in the absence of Coulombic attraction) are most likely a result of high reactivity with amines and excellent stability toward hydrolysis. In particular DSC activation gave rise to a loading level of c.a. 190 ng/cm^2, which is only slightly below the maximum density that can be achieved for a monolayer (i.e., 250 ng/cm^2).[42] Such a functionalization density, although lower than what could be expected for a 3D platform of 30 nm dry thickness (corresponding to nearly 60 nm hydrated thickness), and the moderate size of SA molecules (roughly a 5 nm cube) is not surprising given the high density of polymer brushes and the difficulty that objects (molecules or nanoparticles) have to infiltrate their structure.[34,43] This low infiltration was evidenced by IR and XPS measurements, which show that substantial amounts of DSC reactive moieties remain even after extended incubation times with SA solutions, whereas they fully disappear when incubated with small molecules such as amino-biotin **1**. In comparison, other activating reagents such as nitrophenyl chloroformate, did not give rise to significant SA functionalization, whereas it had been reported to be highly active for small RGD peptide immobilization (results that were independently reproduced by our group).[44]

Effect of PEG Side-Chain Length on Streptavidin Functionalization. Incubation of bt-POEGMA-360 in a SA solution gave rise to fast (the maximum binding plateau is reached within 5 min) protein binding up to a capacity of 460 ng/cm^2. This protein density is in excellent agreement with other studies in which a 530 ng/cm^2 capacity was reported[21] and corresponds to the surface density that would be expected from a SA bilayer. Closely packed SA monolayers would give rise to a surface density of 360 ng/cm^2, however, 2D crystals of these molecules on biotinylated lipid layers displayed well-defined voids,[42] and the resulting protein density decreases to 250 ng/cm^2. Similar monolayers built by direct SA immobilization on biotinylated self-assembled monolayers gave rise to slightly lower densities, in the range of 150−230 ng/cm^2.[45−47] The fast saturation and reproducibility of the SA binding on bt-POEGMA-360 does not support the occurrence of surface precipitation but rather directed immobilization. Hence, protein infiltration must occur to some degree and is favored by the full biotinylation of DSC-activated POEGMA-360.

In comparison, direct SA-functionalization of POEGMA-360 or -526 brushes afforded more moderate protein densities near 190 ng/cm^2. This is likely to be the result of the lower efficiency of DSC coupling, compared to biotin binding (which does not undergo deactivation via hydrolysis). In contrast, SA-immobilization on PHEMA, with its higher density of DSC-activated functions, afforded a protein density of 1.0 μg/cm^2, corresponding to four SA monolayers. This higher biofunctionalization level (higher loading density) is supported by the high nitrogen content measured by XPS and the intensity of the IR amide bands (b and c in Figure S2).

Biotinylated Antibody Binding. Exposure of SA-POEGMA-360 brushes to a solution of bt-Rb-α-Gt gave rise to efficient antibody immobilization with binding capacities near 90 ng/cm^2. The binding saturation is reached in less than 5 min and remains stable, in agreement with the high specificity and association constant of the biotin/SA pair. These moderate binding capacities are presumably a consequence of the large size of antibodies (near 150 kDa) and their difficulty to infiltrate dense architectures such as polymer brushes. This contrasts with platforms where biotinylated proteins and antibodies are immobilized on dense SA SAMs for which binding capacities as high as 200 ng/cm^2 were measured.[46−49] The protein resistance of the PEG-derived brushes used may also contribute to decrease the measured immobilization levels, by reducing nonspecific adsorption.[50] In agreement with these observations, it was shown that smaller biotinylated molecules, such as single strand DNA may infiltrate 3D architectures more easily and give rise to higher binding capacities compared to 2D SA SAMs.[51]

The evolution of the binding capacity toward biotinylated bt-Rb-α-Gt depends on the SA-functionalization level and protein resistance. PHEMA, for which SA immobilization was highest, displayed higher levels of primary antibody binding, near 130 ng/cm^2, whereas levels measured for POEGMA-526 decreased to 43 ng/cm^2. These results are consistent with AGT-fusion protein immobilization capacities reported on brushes presenting a range of benzylguanine densities.[20] Examination of the initial stage of the biotinylated antibody immobilization also suggests that antibodies bind more slowly to PHEMA (which swells less than POEGMA-360) due to slower macromolecule infiltration, even in the upper part of the coating. In contrast to nonbiotinylated brushes, exposure of bt-POEGMA-360 to SA solutions afforded low biotinylated antibody binding (37 ng/cm^2), despite high SA densities, presumably due to saturation of the biotin pockets of immobilized SA molecules.

Secondary Antibody Recognition and Protein Resistance. The recognition of secondary antibodies was insensitive to the type of brush used. The binding capacities varied between 15 and 33 ng/cm^2, with a 2-fold decrease when the PEG side chain length is increased from PHEMA to POEGMA-526. Such binding capacities compare well to those of secondary recognition events reported in the literature for macromolecules of similar sizes (falling between 10 and 50 ng/cm^2).[46,48] In addition, the levels of secondary antibody immobilization measured on biotinylated and SA-functionalized POEGMA-360 brushes are similar, despite a near-3-fold change of biotinylated antibody capacity. These observations suggest that secondary antibodies infiltrate polymer brushes even less than SA and primary biotinylated antibodies: the recognition events occur in the upper part of the brush, where the binding sites of a primary antibody remain accessible to the epitope of a bulky secondary antibody. These observations are consistent with the low and relatively unchanged binding rates (0.6−0.8 ng·cm^{-2} s^{-1}) measured for the different brushes.

Despite displaying recognition properties typical of 2D architectures, the functionalized polymer brushes studied preserved excellent selectivity toward complementary antibodies. This is illustrated by the extremely low binding capacity (near 1 ng/cm^2) measured when a Dk-α-Rt secondary antibody was used for recognition. In addition, fluorescence assays show that dilution of Gt-α-Rt secondary antibodies can be detected using a POEGMA-360 brush down to a concentration of 1 ng/mL in a BSA solution of 10 mg/mL. The protein resistance of polymer brushes decreases markedly when the length of the PEG side chain decreases: the nonspecifically bound protein density for POEGMA brushes is near 15 ng/cm^2 and goes up to 109 ng/cm^2 for PHEMA. Similar changes in protein and cell resistance have been reported.[20,37] These results explain why the trend observed by fluorescence microscopy is different from that determined by SPR. In our fluorescence assay, secondary antibodies were diluted in 10 mg/mL BSA solutions. Therefore, surfaces with low protein resistance will give rise to increased competition between specific recognition and nonspecific binding, which leads to a decrease in the apparent secondary antibody binding capacity.

Conclusion

Owing to their ease of structural and functional design, polymer brushes are attractive synthetic coatings for biofunctionalization. PEG-derived brushes offer the advantage of high protein resistance. The present work established some empirical guidelines for direct protein coupling to neutral antifouling polymer brushes. The ability to functionalize these brushes with a capture protein such as SA results in efficient and selective immobilization platforms that may be used for recognition of specific macromolecules, for medical diagnostic and biofunctional surfaces. It is becoming apparent that molecular recognition and binding capacities may be affected by brush molecular structure and, potentially, packing density. In the example of the dense PEG brushes described, molecular infiltration seems to be dictated by size: small molecules can diffuse throughout the brush (and result in full depth functionalization), whereas bulky antibodies can only bind to moieties present in its upper layer. It can be anticipated that physical parameters such as brush density, heterogeneity, rigidity, and swelling will reveal to be essential parameters to control in order to achieve efficient, selective, and directed immobilization of biomacromolecules.

Acknowledgment. We thank Prof. F. Watt for allowing access to the Leica microscope for fluorescence measurements and Drs. John Connelly and Kim Jensen for discussion of antibody immobilization. The financial support of the Department of Trade and Industry is acknowledged (Technology Strategy Board Grant MNT-0231). J.E.G. thanks Cambridge Cancer Centre for a pilot research award.

Supporting Information Available. Evolution of SA immobilization levels with time and IR spectra for pristine and functionalized PHEMA and POEGMA-526 brushes. This material is available free of charge via the Internet at http://pubs.acs.org.

References and Notes

(1) Homola, J. *Chem. Rev.* **2008**, *108*, 462–493.
(2) Shankaran, D. R.; Gobi, K. V.; Miura, N. *Sens. Actuators, B* **2007**, *121*, 158–177.
(3) Adhikari, B.; Majumdar, S. *Prog. Polym. Sci.* **2004**, *29*, 699–766.
(4) Sheldon, R. A. *Adv. Synth. Catal.* **2007**, *349*, 1289–1307.
(5) Reetz, M. T.; Zonta, A.; Simpelkamp, J. *Angew. Chem., Int. Ed.* **1995**, *34*, 301–303.
(6) Fink, J.; Thery, M.; Azioune, A.; Dupont, R.; Chatelain, F.; Bornens, M.; Piel, M. *Lab Chip* **2007**, *7*, 672–680.
(7) Falconnet, D.; Csucs, G.; Grandin, H. M.; Textor, M. *Biomaterials* **2006**, *27*, 3044–3063.
(8) Torrance, L.; Ziegler, A.; Pittman, H.; Paterson, M.; Toth, R.; Eggleston, I. *J. Virol. Methods* **2006**, *134*, 164–170.
(9) Davies, J.; Roberts, C. J.; Dawkes, A. C.; Sefton, J.; Edwards, J. C.; Glasbey, T. O.; Haymes, A. G.; Davies, M. C.; Jackson, D. E.; Lomas, M.; Shakesheff, K. M.; Tendler, S. J. B.; Wilkins, M. J.; Williams, P. M. *Langmuir* **1994**, *10*, 2654–2661.
(10) Sigal, G. B.; Bamdad, C.; Barberis, A.; Strominger, J.; Whitesides, G. M. *Anal. Chem.* **1996**, *68*, 490–497.
(11) Dai, J.; Bao, Z.; Sun, L.; Hong, S. U.; Baker, G. L.; Bruening, M. L. *Langmuir* **2006**, *22*, 4274–4281.
(12) Prime, K. L.; Whitesides, G. M. *J. Am. Chem. Soc.* **1993**, *115*, 10714–10721.
(13) Marinakos, S. M.; Chen, S.; Chilkoti, A. *Anal. Chem.* **2007**, *79*, 5278–5283.
(14) Jones, D. M.; Brown, A. A.; Huck, W. T. S. *Langmuir* **2002**, *18*, 1265–1269.
(15) Edmondson, S.; Osborne, V. L.; Huck, W. T. S. *Chem. Soc. Rev.* **2004**, *33*, 14–22.
(16) Brown, A. A.; Khan, N. S.; Steinbock, L.; Huck, W. T. S. *Eur. Polym. J.* **2005**, *41*, 1757–1765.
(17) Ma, H.; Hyun, J.; Stiller, P.; Chilkoti, A. *Adv. Mater.* **2004**, *16*, 338–341.
(18) O'Shannessy, D. J.; Burke, M. B.; Peck, K. *Anal. Biochem.* **1992**, *205*, 132–136.
(19) Glinel, K.; Jonas, A. M.; Jouenne, T.; Leprince, J.; Galas, L.; Huck, W. T. S. *Bioconjugate Chem.* **2009**, *20*, 71–77.
(20) Tugulu, S.; Arnold, A.; Sielaff, I.; Johnsson, K.; Klok, H.-A. *Biomacromolecules* **2005**, *6*, 1602–1607.
(21) Lee, B. S.; Chi, Y. S.; Lee, K.-B.; Kim, Y.-G.; Choi, I. S. *Biomacromolecules* **2007**, *8*, 3922–3929.
(22) Lee, B. S.; Lee, J. K.; Kim, W.-J.; Jung, Y. H.; Sim, S. J.; Lee, J.; Choi, I. S. *Biomacromolecules* **2007**, *8*, 744–749.
(23) Wilchek, M.; Bayer, E. A. *Anal. Biochem.* **1988**, *171*, 1–32.
(24) Yokoyama, K.; Leigh, B. S.; Sheng, Y.; Niki, K.; Nakamura, N.; Ohno, H.; Winkler, J. R.; Gray, H. B.; Richards, J. H. *Inorg. Chim. Acta* **2008**, *361*, 1095–1099.
(25) Iglesias, L. E.; Baldessari, A.; Gros, E. G. *Org. Prep. Proced. Int.* **1996**, *28*, 319–324.
(26) Jones, D. M.; Smith, J. R.; Huck, W. T. S.; Alexander, C. *Adv. Mater.* **2002**, *14*, 1130–1134.
(27) Zhou, F.; Zheng, Z.; Yu, B.; Liu, W.; Huck, W. T. S. *J. Am. Chem. Soc.* **2006**, *128*, 16253–16258.
(28) de Vos, W. M.; Biesheuvel, P. M.; de Keizer, A.; Kleijn, J. M.; Cohen Stuart, M. A. *Langmuir* **2008**, *24*, 6575–6584.
(29) Abuchowski, A.; van Es, T.; Palczuk, N. C.; Davis, F. F. *J. Biol. Chem.* **1977**, *252*, 3578–3581.
(30) Roberts, M. J.; Bentley, M. D.; Harris, J. M. *Adv. Drug Delivery Rev.* **2002**, *54*, 459–476.
(31) Francis, G. E.; Fisher, D.; Delgado, C.; Malik, F.; Gardiner, A.; Neale, D. *Int. J. Hematol.* **1998**, *68*, 1–18.
(32) Diamanti, S.; Arifuzzaman, S.; Elsen, A.; Genzer, J.; Vaia, R. A. *Polymer* **2008**, *49*, 3770–3779.

(33) Yoshikawa, C.; Goto, A.; Tsujii, Y.; Fukuda, T.; Kimura, T.; Yamamoto, K.; Kishida, A. *Macromolecules* **2006**, *39*, 2284–2290.
(34) Yoshikawa, C.; Goto, A.; Tsujii, Y.; Ishizuka, N.; Nakanishi, K.; Fukuda, T. *J. Polym. Sci., Part A: Polym Chem.* **2007**, *45*, 4795–4803.
(35) Lahiri, J.; Ostuni, E.; Whitesides, G. M. *Langmuir* **1999**, *15*, 2055–2060.
(36) Beamson, G.; Briggs, D. High resolution XPS of organic polymers. *The Scienta ESCA300 database*; John Wiley and Sons: Chichester, 1992.
(37) Fan, X.; Lin, L.; Messersmith, P. B. *Biomacromolecules* **2006**, *7*, 2443–2448.
(38) Liedberg, B.; Lundstrom, I.; Stenberg, E. *Sens. Actuators, B* **1993**, *11*, 63–72.
(39) Vaisocherova, H.; Yang, W.; Zhang, Z.; Cao, Z.; Cheng, G.; Piliarik, M.; Homola, J.; Jiang, S. *Anal. Chem.* **2008**, *80*, 7894–7901.
(40) Vaisocherova, H.; Zhang, Z.; Yang, W.; Cao, Z.; Cheng, G.; Taylor, A. D.; Piliarik, M.; Homola, J.; Jiang, S. *Biosens. Bioelectron.* **2009**, *24*, 1924–1930.
(41) Jain, P.; Sun, L.; Dai, J.; Baker, G. L.; Bruening, M. L. *Biomacromolecules* **2007**, *8*, 3102–3107.
(42) Darst, S. A.; Ahlers, M.; Meller, P. H.; Kubalek, E. W.; Blankenburg, R.; Ribi, H. O.; Ringsdorf, H.; Kornberg, R. D. *Biophys. J.* **1991**, *59*, 387–396.
(43) Oren, R.; Liang, Z.; Barnard, J. S.; Warren, S. C.; Wiesner, U.; Huck, W. T. S. *J. Am. Chem. Soc.* **2009**, *131*, 1670–1671.
(44) Tugulu, S.; Silacci, P.; Stergiopulos, N.; Klok, H.-A. *Biomaterials* **2007**, *28*, 2536–2546.
(45) Jung, L. S.; Nelson, K. E.; Stayton, P. S.; Campbell, C. T. *Langmuir* **2000**, *16*, 9421–9432.
(46) Choi, S. H.; Lee, J. W.; Sim, S. J. *Biosens. Bioelectron.* **2005**, *21*, 378–383.
(47) Chelmowski, R.; Prekelt, A.; Grunwald, C.; Woll, C. *J. Phys. Chem.* **2007**, *111*, 12295–12303.
(48) Saerens, D.; Frederix, F.; Reekmans, G.; Conrath, K.; Jans, K.; Brys, L.; Huang, L.; Bosmans, E.; Maes, G.; Borghs, G.; Muyldermans, S. *Anal. Chem.* **2005**, *77*, 7547–7555.
(49) Lee, J. W.; Sim, S. J.; Cho, S. M.; Lee, J. *Biosens. Bioelectron.* **2005**, *20*, 1422–1427.
(50) Uchida, K.; Otsuka, H.; Kaneko, M.; Kataoka, K.; Nagasaki, Y. *Anal. Chem.* **2005**, *77*, 1075–1080.
(51) Yang, N.; Su, X.; Tjong, V.; Knoll, W. *Biosens. Bioelectron.* **2007**, *22*, 2700–2706.

BM900706R